Corium materials characterizations through electron microscopy and X-ray diffraction

Emmanuelle Brackx, Mohamed Jizzini, Hirotomo Hikeuchi, P Piluso, René Guinebretière

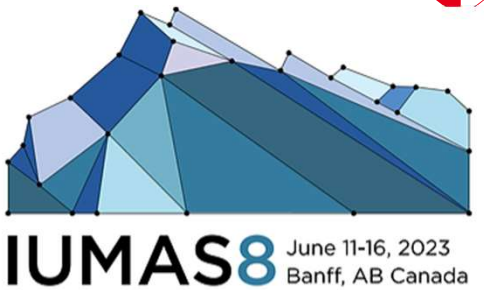

Corium materials characterizations through electron microscopy and X ray diffraction

Emmanuelle Brackx[1], Mohamed Jizzini[1,2], Hirotomo Hikeuchi[3], Pascal Piluso[4], René Guinebretière[2]

[1] CEA, DES, ISEC, DMRC, Univ. Montpellier, Marcoule, France

[2] IRCER, Univ. Limoges, Limoges, France

[3] JAEA, 4-33 Muramatsu, Tokai-mura, Ibaraki-ken, Japan

[4] CEA, DES, IRESNE, DTN, Saint Paul lez Durance, France

IUMAS, 11-16 June 2023

Corium formation with the severe nuclear accidents

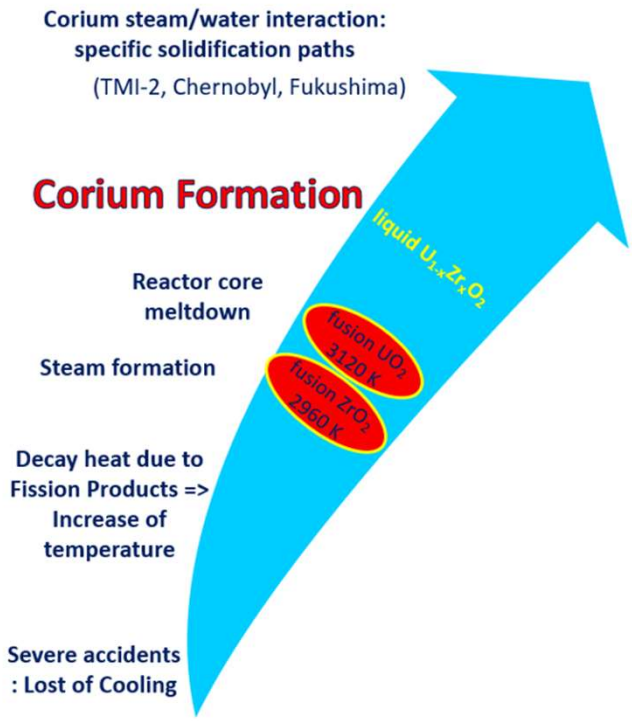

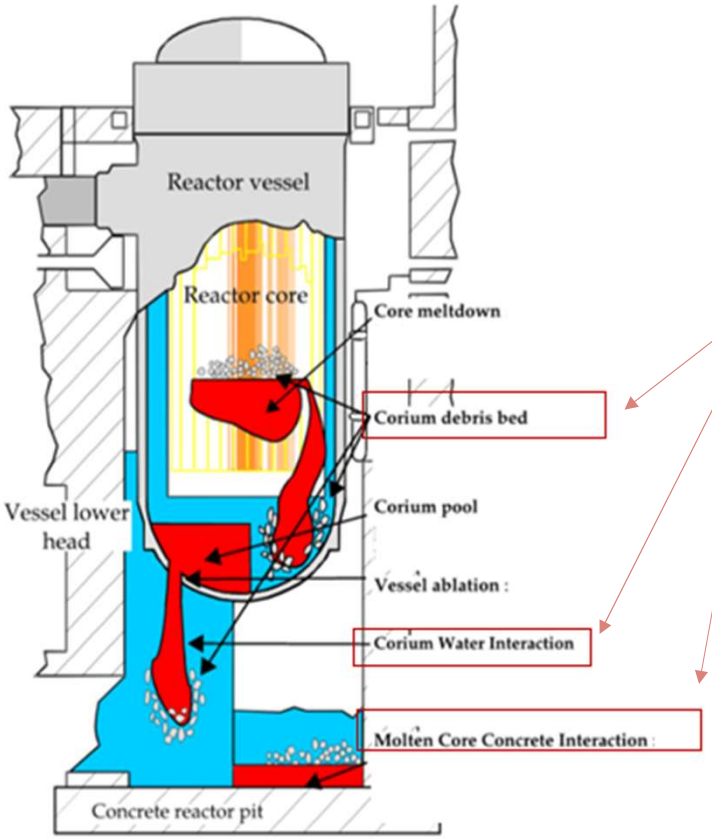

3 study parts

Study on the distribution of boron in the in-vessel fuel debris

- Study on the distribution of boron in the in-vessel fuel debris in conditions close to Fukushima Daiichi Nuclear Power Station Unit 2

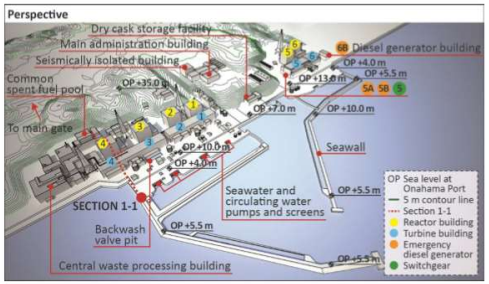

- To evaluate carefully the potential risk of re-criticality during decommissioning of the Fukushima Daiichi NPS (1F).

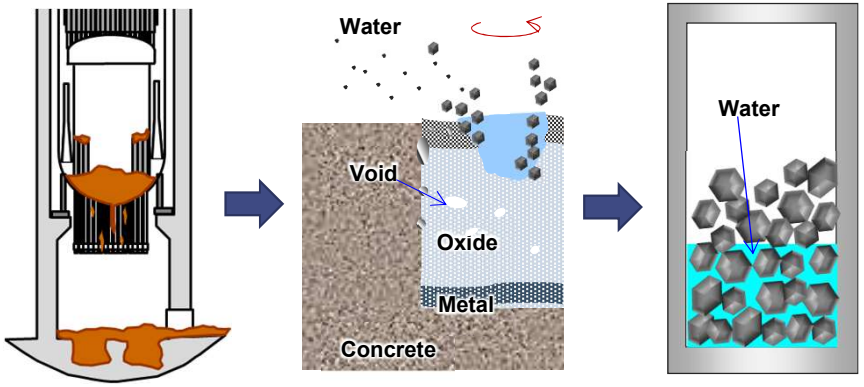

Formation of fuel debris

Debris retrieval (core-boring)

Storage (without drying)

- Chemical forms of B in fuel debris is scenario dependent.
  - ✓ Material composition
  - ✓ Temperature history
  - ✓ Red-ox condition

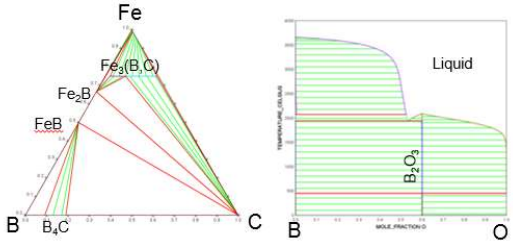

Study on the distribution of boron in the in-vessel fuel debris

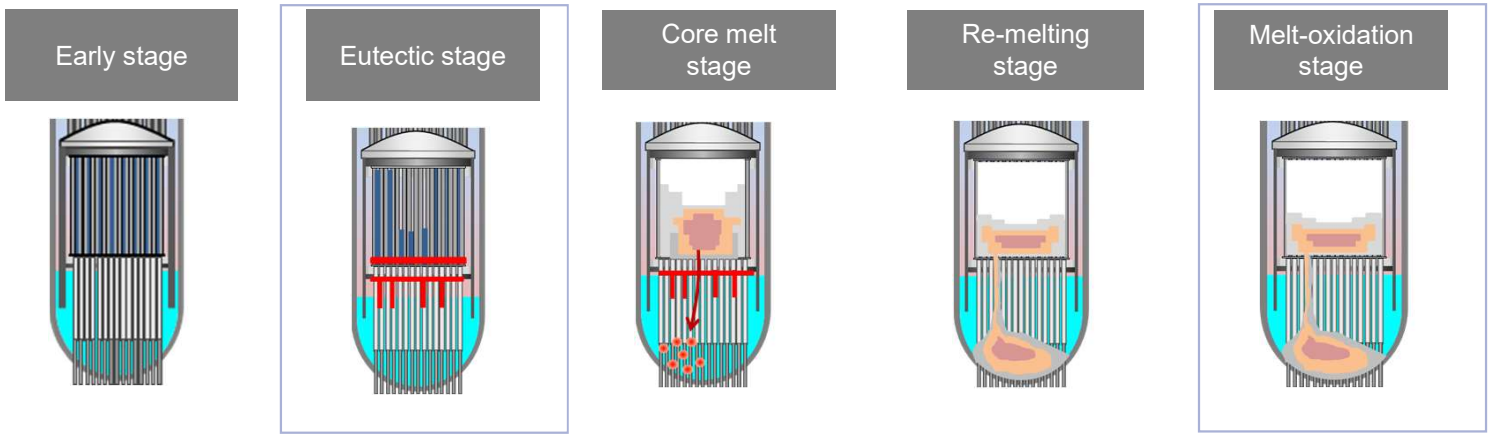

Test No.	JVT-B1	JVT-B3	JVT-B4
Elemental system (Case assumed)	B-Fe-O (The melt-oxidation stage)	B-C-Fe-O (The eutectic stage)	
Loaded raw materials $Fe/Fe_2O_3/B_4C/B_2O_3$	47.537 / 0 / 0 / 1.393 in gram	60.353 / 1.137 / 2.134 / 0 in gram	60.640 / 1.142 / 2.144 / 0 in gram
Atomic fraction of B/C/Fe/O	0.0421 / 0 / 0.8948 / 0.0631	0.1180 / 0.0295 / 0.8362 / 0.0163	
Cooling condition	**Rapid** cooling (~10^2 K/min)	**Rapid** cooling (~10^2 K/min)	**Slow** cooling (~10 K/min)

- Solidification tests on melt of B-C-Fe-O system
- Heat treatment in PLINIUS/VITI facility

Study on the distribution of boron in the in-vessel fuel debris

- EPMA Light element analysis B-C-O.
- **X- ray generation and emission of the light elements take place in extremely shallow surface volumes under the specimen surface.**
- Carefully to the specimen preparation, used an anticontamination device

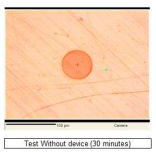

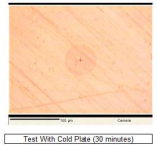

Chemical shift of boron and carbon

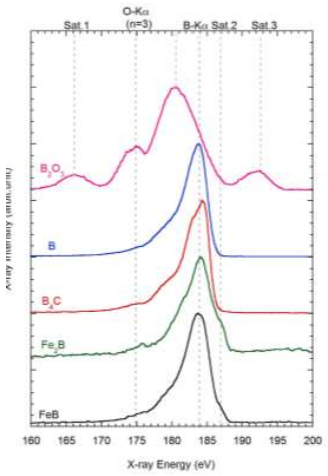

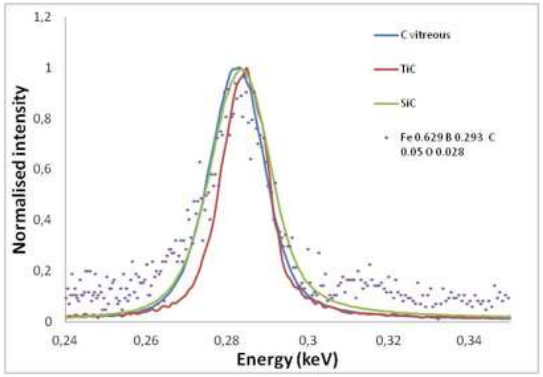

- XRD phases analysis.

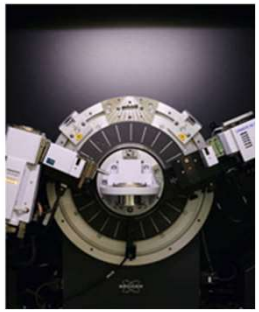

Study on the distribution of boron in the in-vessel fuel debris

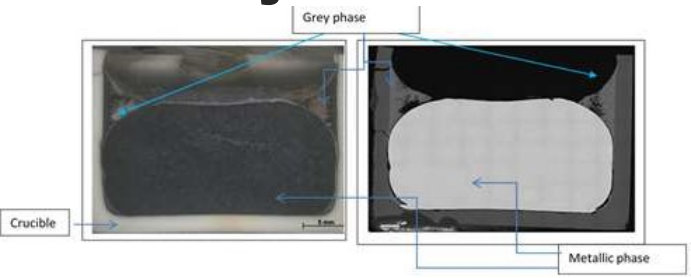

JVT-B1

Metallic/Oxidic phases identified

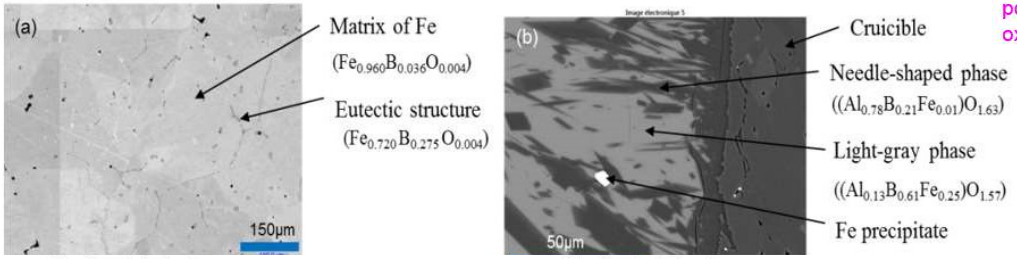

JVT-B3

JVT-B4

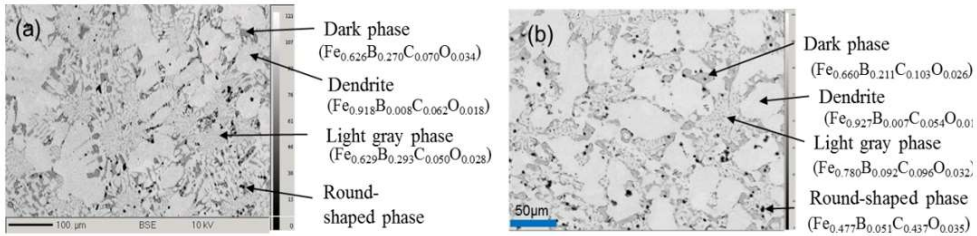

Both test showed eutectic structure with B-C-O-Fe system.

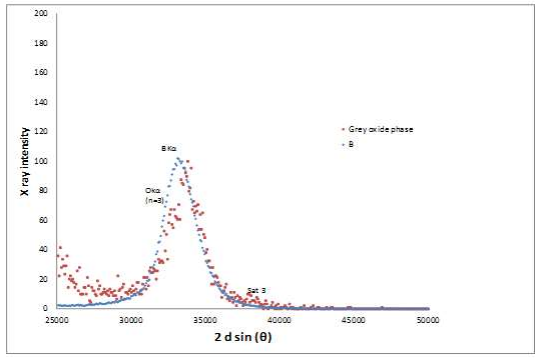

Influence of the chemical bond on the shape and position of the emission line measured on the grey oxide phase.

- B_2O_3 solid can be formed at temperatures from 450°C to 500 °C.
- Around 1150 °C-1200°C, a liquid containing melted Fe_3 (B, C) and Fe_2B eutectic phases is formed.
- Fe-B-C hypo eutectic alloy solidification begins by a heterogeneous nucleation of the primary gamma-Fe phase with the formation of dendrites, while the residual melt is enriched in elements combining C and B.
- XRD analysis confirmed the formation of this phases.

Summary

-Formation of boride and boron-carbides of Fe, and the oxide phase rich in B_2O_3 were clearly indicated.
-The observed phases can be reproduced by appropriate modeling by JAEA.

Corium-water (ICE) interaction/vapour explosion and prototypical corium formation U1-xZrxO2±y

PLINIUS:
Experimental platform, located at the CEA Cadarache site

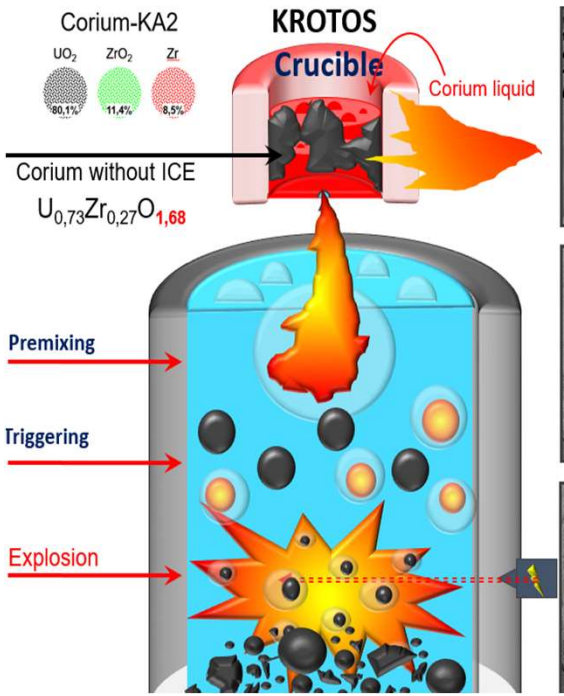

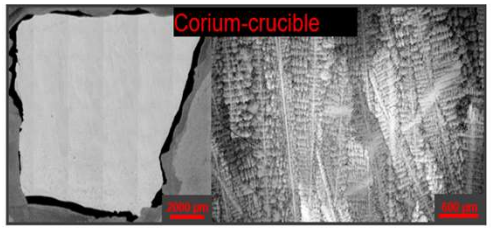

Residual material located into the crucible after the samples elaboration (a few minutes)

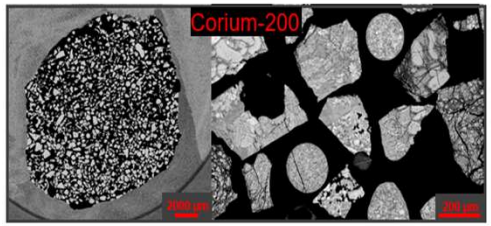

Corium powder formed after interaction with water: Pre-mixing, triggering, propagation without explosion (a few seconds)

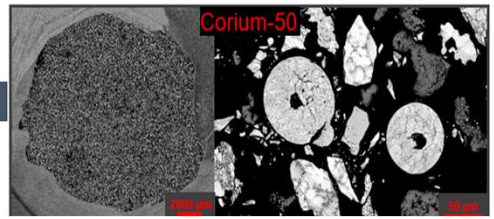

Corium powder formed after interaction with water: Premixing, triggering, propagation then explosion (a few milliseconds).

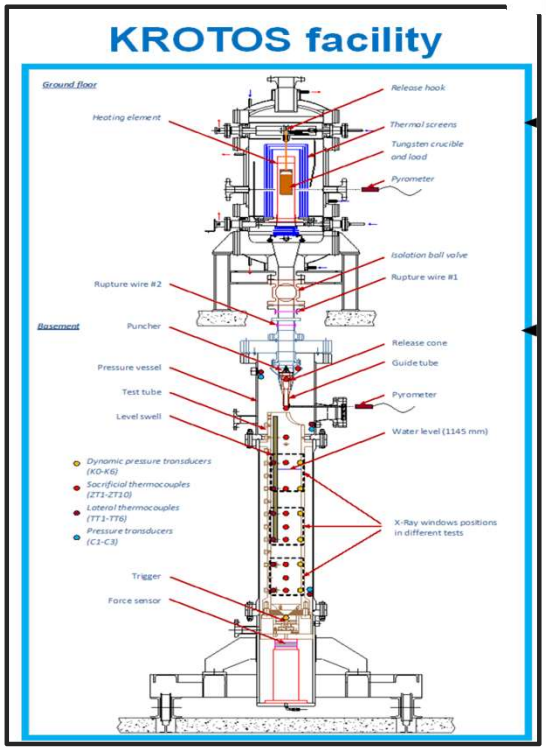

Interpretation of asymmetric widening of diffraction lines

XRD in laboratory:

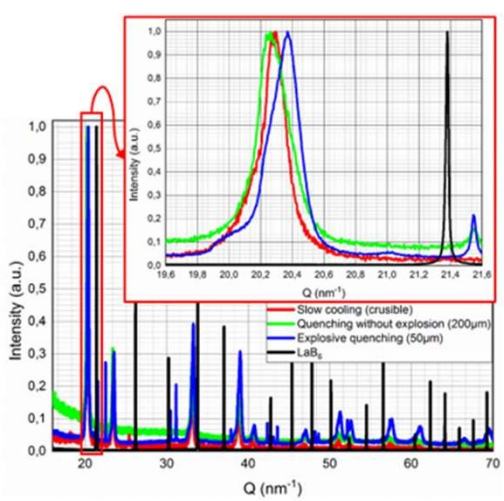

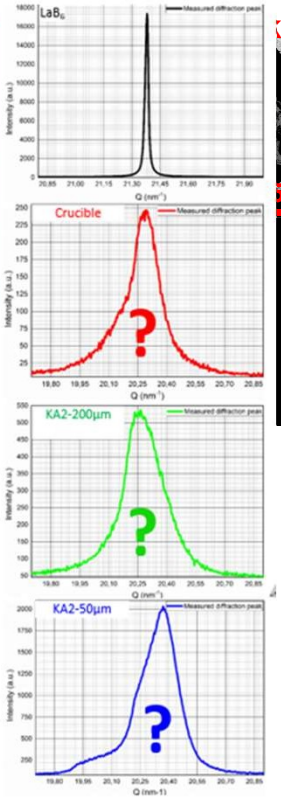

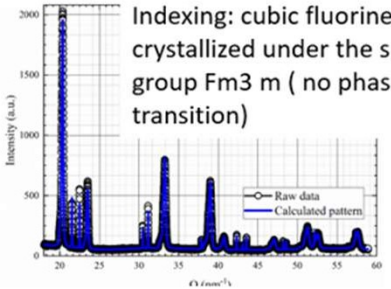

Indexing: cubic fluorine phase crystallized under the spatial group Fm3 m (no phase transition)

Microstructural study of corium KA2 by SEM EBSD

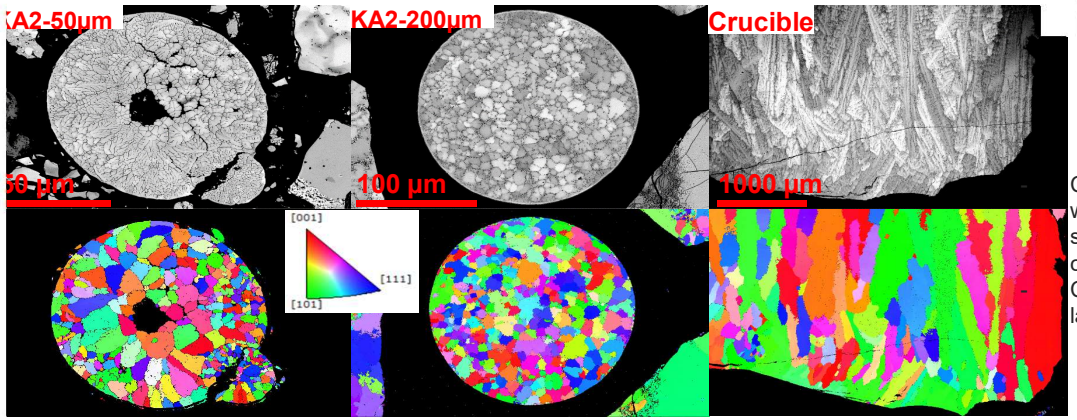

Crystal size decreases with decreasing particle size and increasing cooling rate.
Crystal size is much larger than micrometer.

- ✓ Very large asymmetric enlargement in relation to instrumental function
- ✓ Only one cubic phase of the space group Fm3 m, whose cationic compositions vary (no phase transition)
- ✓ Cationic fluctuation in cubic solid solutions crystallised under the spatial group $Fm\bar{3}m$
- ✓ The simultaneous presence of several compositions whose mesh parameters vary with the difference in U/ Zr or/and oxygen content

$$U_{1-x}Zr_xO_{2\pm y}$$

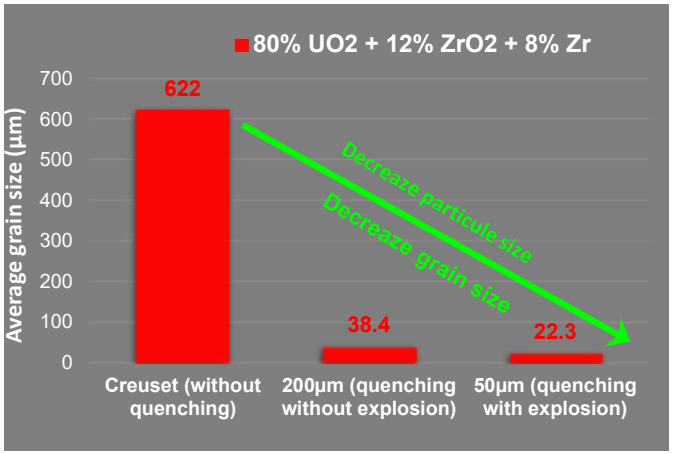

Structural analysis by X-ray and neutron diffraction

X-ray diffraction on the MARS beam line at the SOLEIL synchrotron:
study of fluctuations in cationic composition

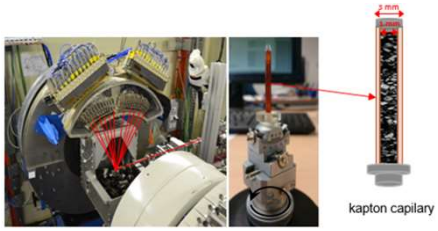

MARS beam line SOLEIL synchrotron CX2 station:
HR-XRD station equipped with 24 crystal analyzers.

The instrumental resolution function: (λ = 0,7276 Å)
Diffraction diagram collected on LaB_6 standard powder

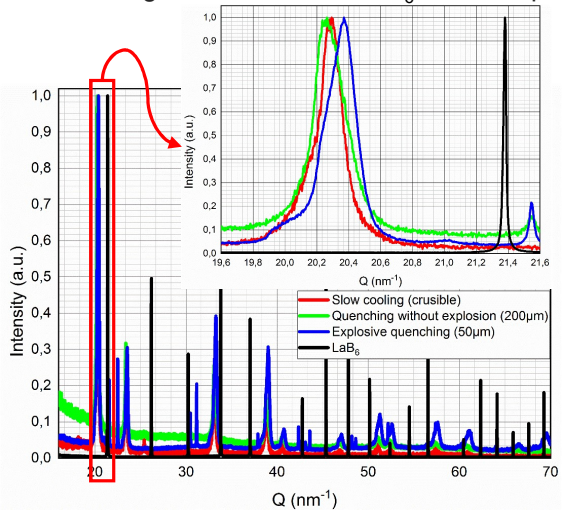

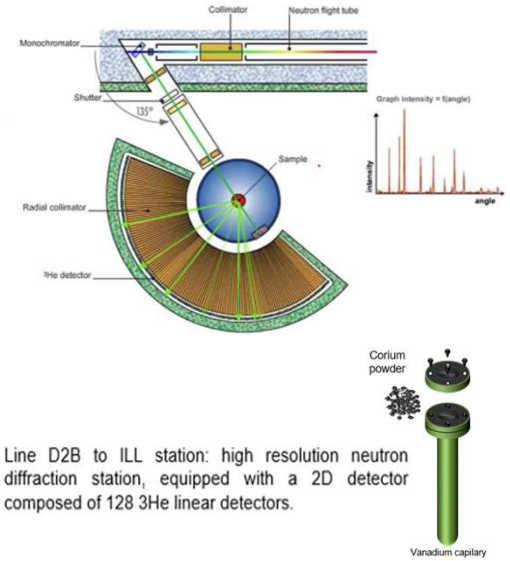

Line D2B to ILL station: high resolution neutron diffraction station, equipped with a 2D detector composed of 128 3He linear detectors.

Neutron diffraction on line D2B to ILL:
study of anionic composition, oxygen stoichiometry

The instrumental resolution function: (λ = 1,5941 Å)
Diffraction diagram collected on $Na_2Ca_3Al_2F_{14}$ standard powder

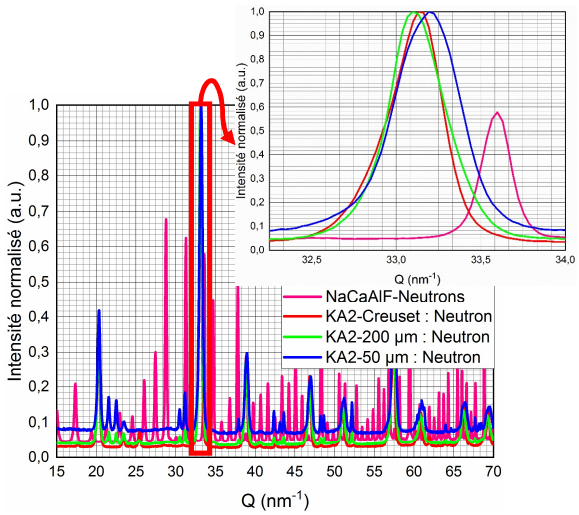

Application of the decomposition method on prototypical corium

- Decomposition of a peak profile with a strong asymmetric broadening characteristic of a cationic composition distribution, into a series of N elementary peaks.
- The mathematical function and the shape parameters are obtained from a standard (LaB6).
- Each elemental peak represents a particular cationic composition.

MAUD: Materials Analysis Using Diffraction

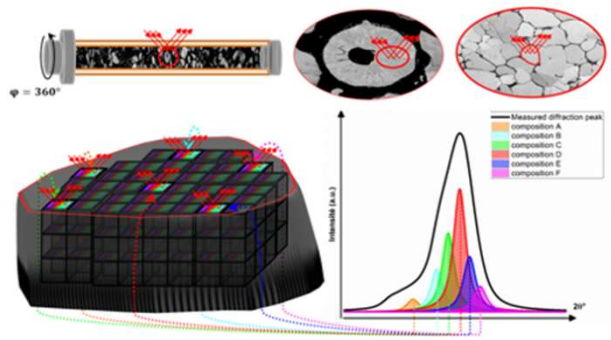

Choice of N elementary peaks:

$$N \approx \frac{\text{full width } of\, U_{1-x}Z_xO_{2\pm y}}{FWHM\ du\ LaB_6}$$

Choice of N elementary cationic compositions:

Vegard Low : $a = 5{,}468 - 0{,}3296\ x$

$\mathbf{0} < x < \mathbf{0{,}57}\ ;\ \Delta x = \mathbf{0{,}02}$

$5{,}46800 < a < 5{,}28013\ ;\ \Delta a = 0{,}006592$

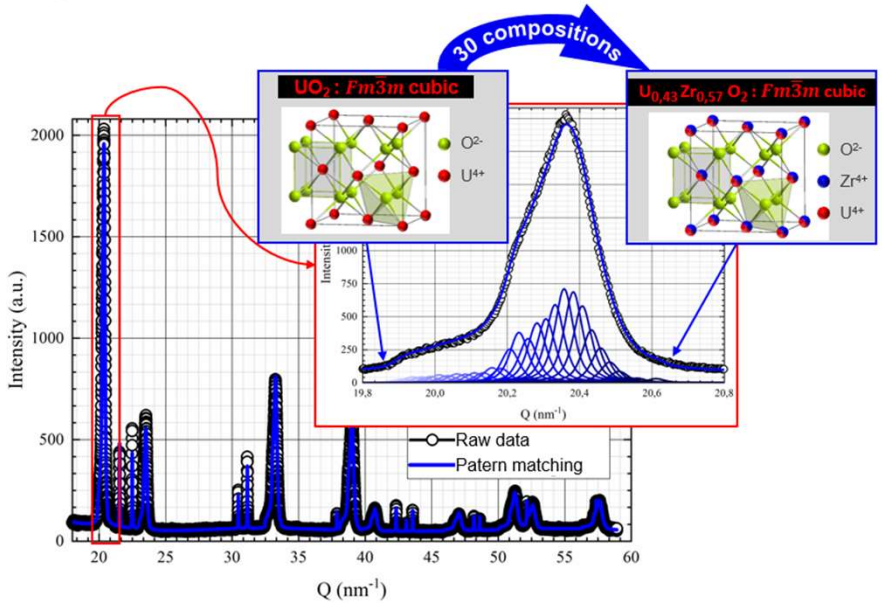

- Extraction of composition fluctuations by global simulation of diffraction diagrams.
- The calculated diagram is the sum of 30 contributions, each corresponding to a given composition.

Quantification of the fluctuation of cation compositions and oxygen content by combined Rietveld X-ray and neutron diffraction analysis

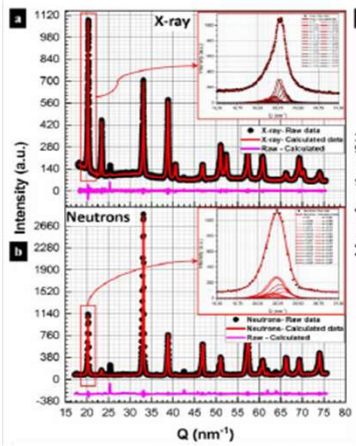

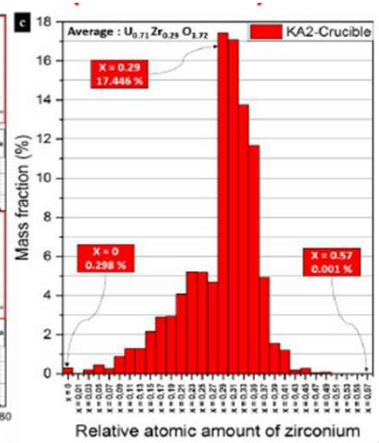

Corium solid solution $U_{1-x}Zr_xO_{2\pm y}$	KA2-Crucible			KA2-200			KA2-50		
Atome	U_{1-x}	Zr_x	$O_{2\pm y}$	U_{1-x}	Zr_x	$O_{2\pm y}$	U_{1-x}	Zr_x	$O_{2\pm y}$
B_{iso} (Å²)	0,324		0,636	0,319		0,915	0,363		1,598
microstrain (%)	0,08			0,09			0,1		
Composition with combinated diffraction (neutrons-X rays)	$U_{0,71}Zr_{0,29}O_{1,72}$			$U_{0,66}Zr_{0,34}O_{1,78}$			$U_{0,64}Zr_{0,36}O_{1,82}$		
Composition with EPMA microanalysis	$U_{0,58}Zr_{0,42}O_{1,88}$			$U_{0,6}Zr_{0,4}O_{1,79}$			$U_{0,63}Zr_{0,37}O_{1,83}$		
R_B	4,27			3,72			4,44		
R_{wp}	6,42			5,45			6,56		
R_{exp}	9,31			10,81			10,20		

→ **Combined Rietveld analysis with X ray and neutron diffraction accurate the determination of solid solution, this result are in good agreement with local EPMA microanalysis realized in the sample.**

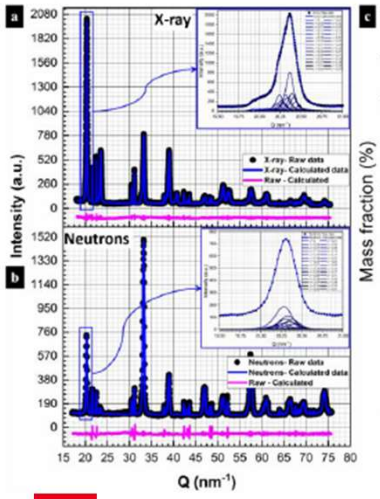

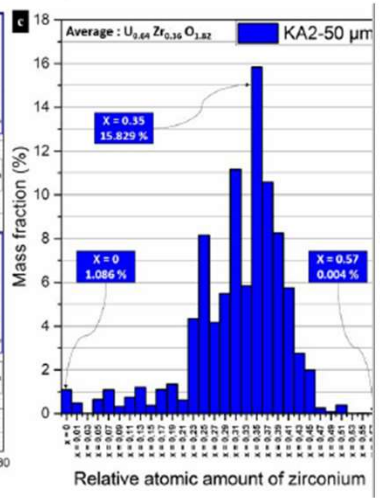

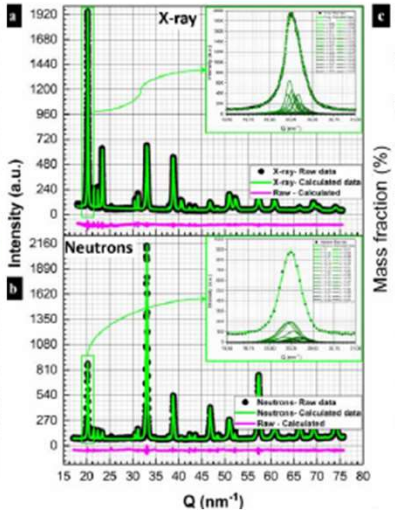

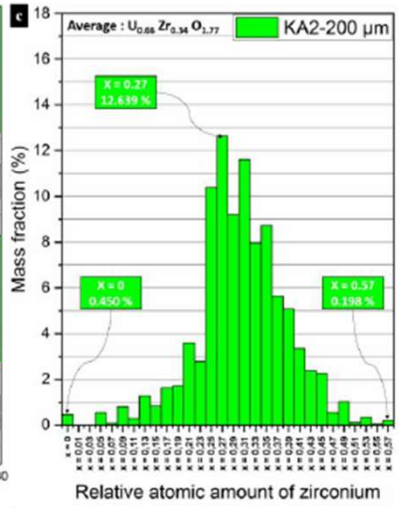

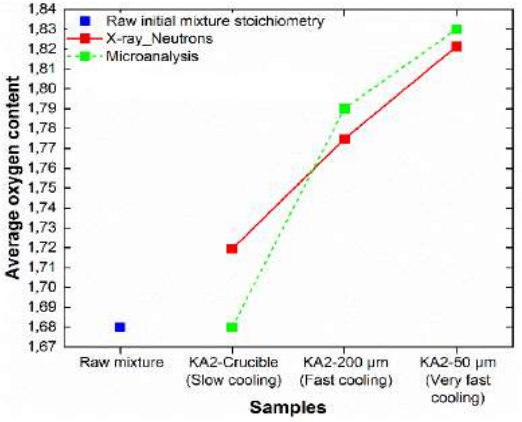

Local deformations analysis by µ Laue diffraction

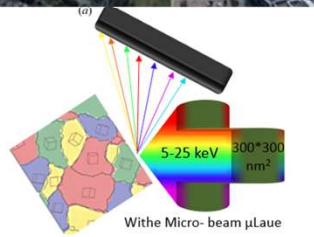

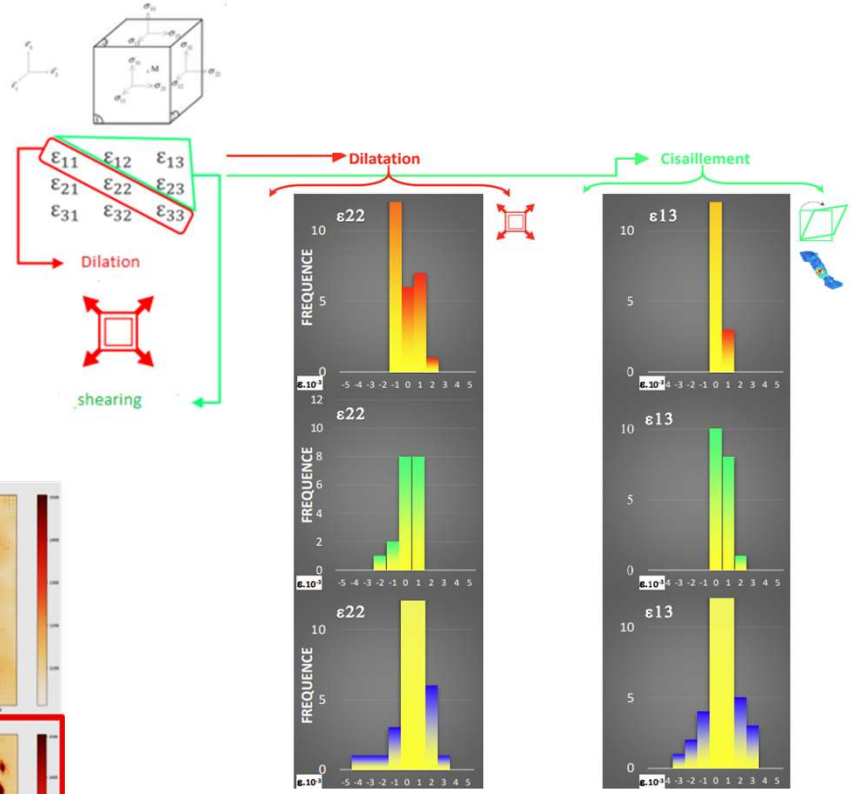

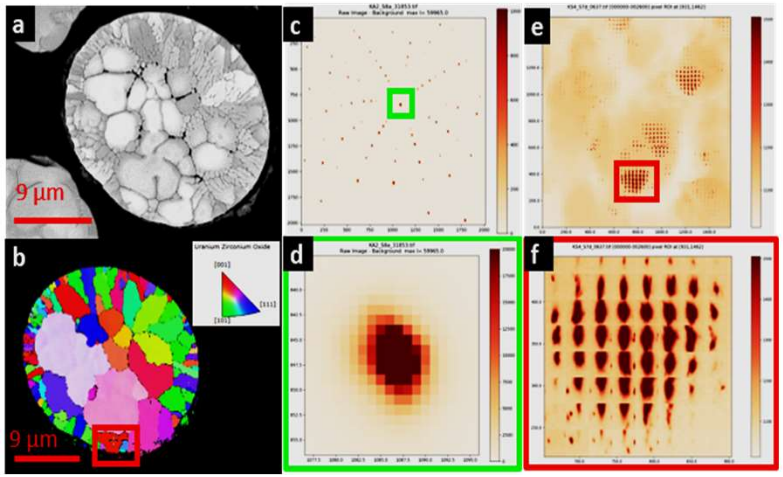

→ **LAUE micro-diffraction : Interplay between composition fluctuations and stresses into crystals of uranium-zirconium and can show an increase of local deformation rate with the fast cooling.**

KA2-Crucible: local deformation rate 0.1 %

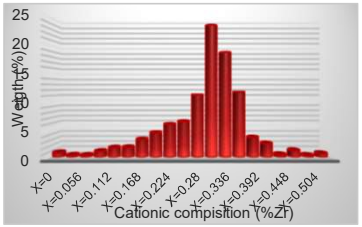

KA2-200µm: local deformation rate 0.2 %

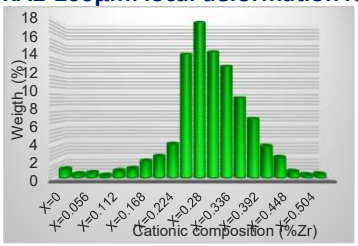

KA2-50µm: local deformation rate 0.3 %

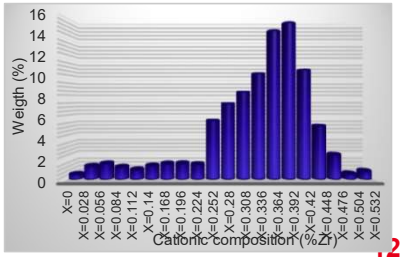

Corium-concrete interaction

A sample of prototypic concrete corium was prepared at the SICOPS AREVA G facility in Germany in order to follow an inter-laboratory comparison test round robin

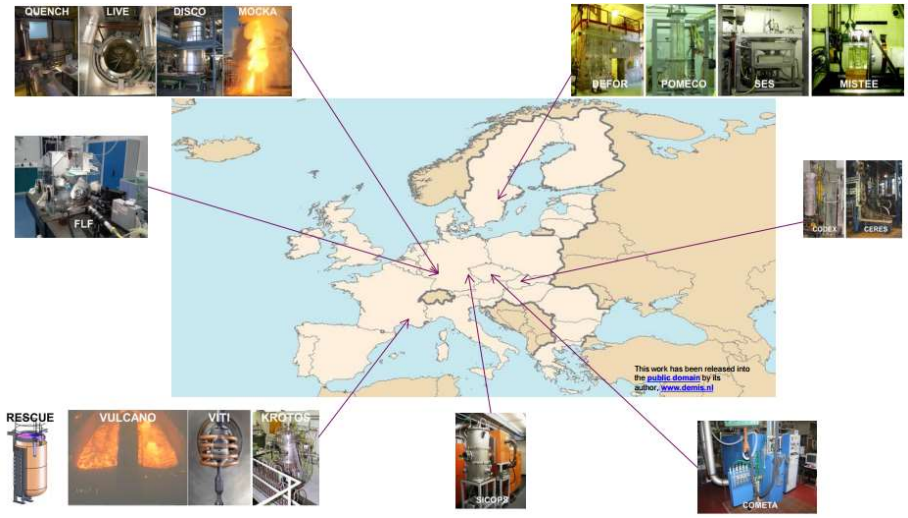

SAFEST partner experimental platforms for studying Corium

→ **4 area was investigate by EPMA in SAFEST MCCI sample**

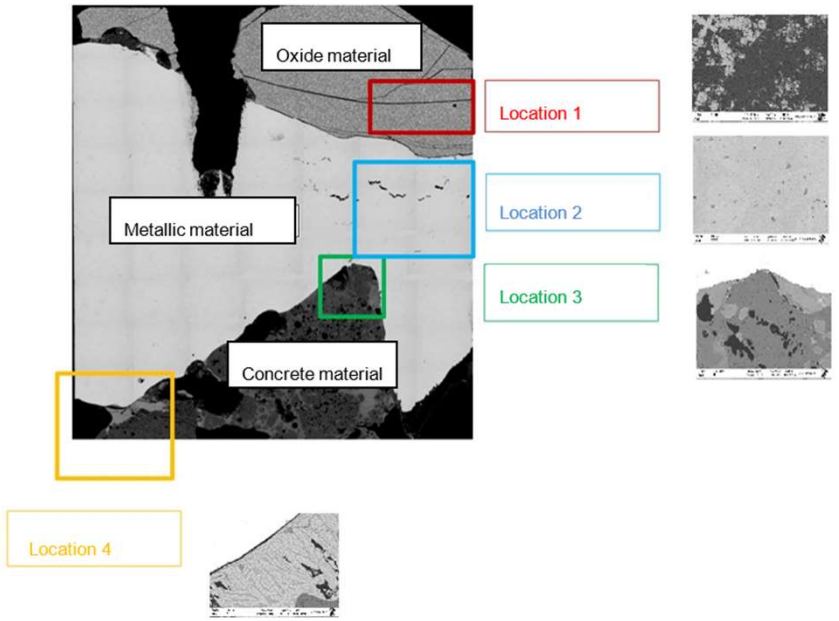

Corium-concrete interaction

→ Location 1: oxide zone

	O (wt%)	O (σwt%)	Na (wt%)	Na (σwt%)	Al (wt%)	Al (σwt%)	Si (wt%)	Si (σwt%)	K (wt%)	K (σwt%)	Ca (wt%)	Ca (σwt%)	Fe (wt%)	Fe (σwt%)	Zr (wt%)	Zr (σwt%)	U (wt%)	U (σwt%)	S (wt%)	S (σwt%)	Mg (wt%)	Mg (σWt%)	Total (Wt%)
Phase dendritique (1)	13.16	0.13											0.57	0.17	9.13	0.54	75.86	1.21					98.74
Phase sombre (2)	42.55	0.44	0.31	0.06	2.36	0.05	28.00	0.17	0.80	0.07	7.16	0.20	13.38	0.49	3.68	0.38	2.11	0.32	0.02	0.03	0.17	0.02	100.54
Analyse globale zone oxyde	38.83	0.41	0.24	0.06	1.55	0.04	17.26	0.13	0.64	0.08	5.37	0.17	10.12	0.41	8.59	0.55	15.60	0.73	0.00	0.04			98.21
phase circulaire (3)	0.12	0.03											99.15	1.79									99.27

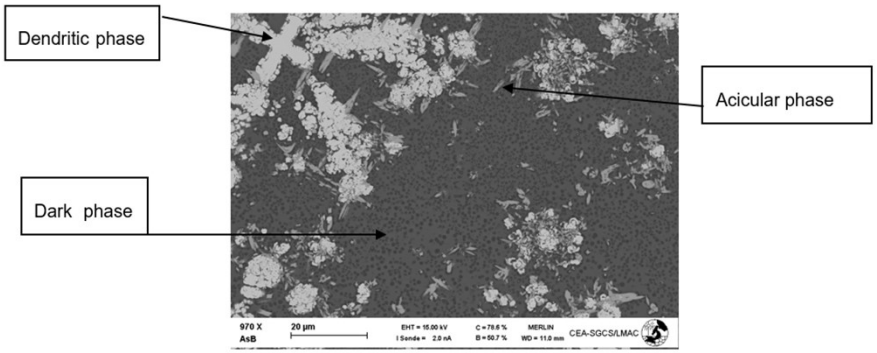

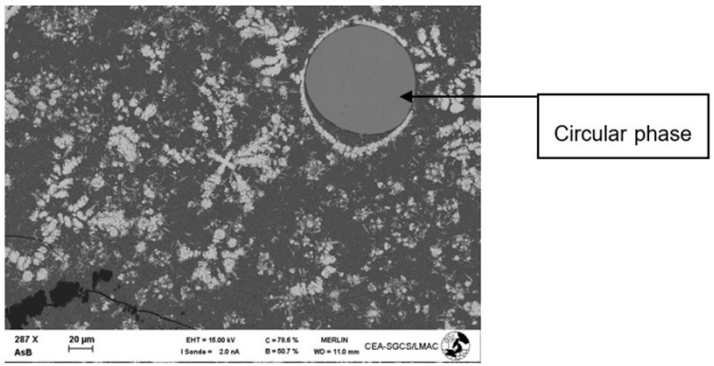

The dendritic phases consist of a mixed U-Zr-Fe-O type oxide, because of the total solubility of UO_2 and ZrO_2 and the insertion of traces of Fe.

The dark phase measured is a U-Zr-Fe-Ca-Si-Al-O type. The formation of this phase could be due to interaction with the concrete at high temperature.

The circular phases represent a pure iron phase with a thin layer of oxide on the surface.

Corium-concrete interaction

→ **Location 2: metallic zone**

Phase	O (wt%)	O (σwt%)	Fe (wt%)	Fe (σwt%)	S (wt%)	S (σwt%)	P (wt%)	P (σwt%)	C (wt%)	C (σwt%)	N (wt%)	N (σwt%)	Total (wt%)
Metallic	0.05	0.03	99.88	1.67	0.05	0.03	0.04	0.03	0.42	0.08	0.08	0.01	100.51
Précipitate	0.14	0.04	64.67	1.21	34.82	0.56							99.63

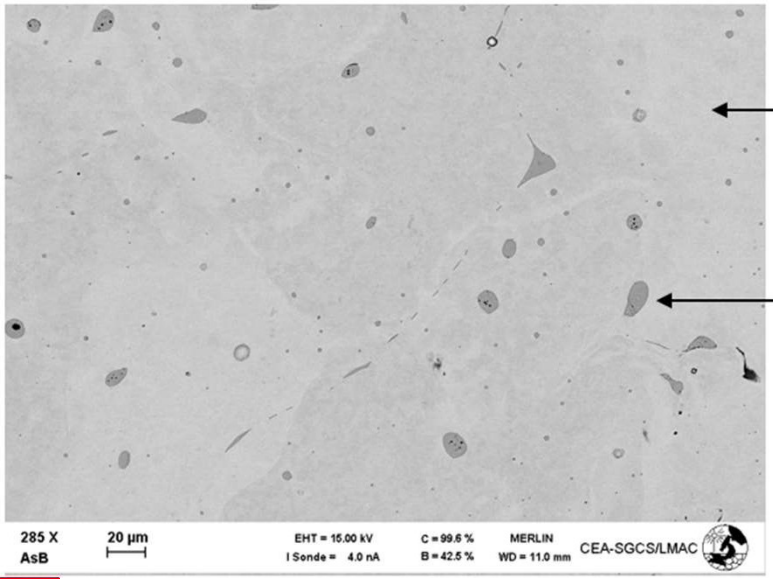

Special sample preparation technique using a carbon anti-contamination cold trap. The analysis results show significant values for the trace elements S, C, and P. The steel measured could be similar to a 37-2 steel, which contains sulfur.

In the metallic phase, FeS-type precipitates dominate, while two other randomly-scattered types Fe_3S_2 and Fe_3S of precipitate phase could also be measured. The formation of these precipitates can be explained if sulfur was included as an additive in the steel at the outset.

Corium-concrete interaction

→ Location 3: metallic/concrete zone

	O (wt%)	O (σwt	Na (wt%)	Na (σwt%)	Al (wt%	Al (σwt%)	Si (wt%)	Si (σwt	K (wt%)	K (σwt%)	Ca (wt%)	Ca (σwt	Fe (wt%)	Fe (σwt%	Zr (wt%	Zr (σwt%)	U (wt%)	U (σwt%)	S (wt%	S (σwt%	Mg (wt%)	Mg (σwt	P (wt%)	P (σwt%)	Total (wt%)
Global area of light grey phase	46.21	0.47	0.61	0.07	3.58	0.06	34.08	0.19	2.29	0.11	5.07	0.17	7.37	0.36	0.14	0.13	-0.02	0.26	0.02	0.04	0.22	0.02	0.02	0.02	99.47
light grey phase in the border	44.06	0.45	0.53	0.08	3.58	0.06	31.66	0.18	1.57	0.09	6.98	0.20	11.60	0.45	0.30	0.13	0.41	0.24	0.08	0.04					100.77

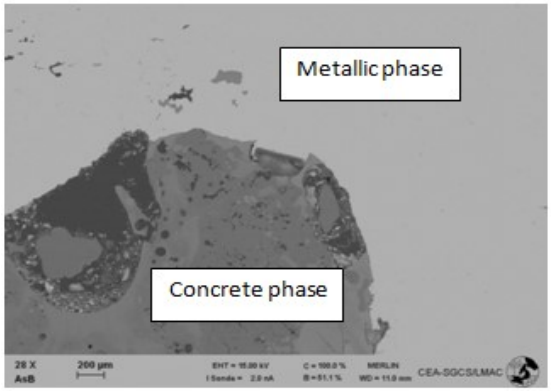

This complex corium phase was measured using average zones with 10 µm dimensions. They show that this is a U-Zr-Fe-Ca-Si-Al-O type corium phase with low uranium content.

The light border phase show that they are enriched in Fe.

Corium-concrete interaction

Location 4: metallic/concrete zone

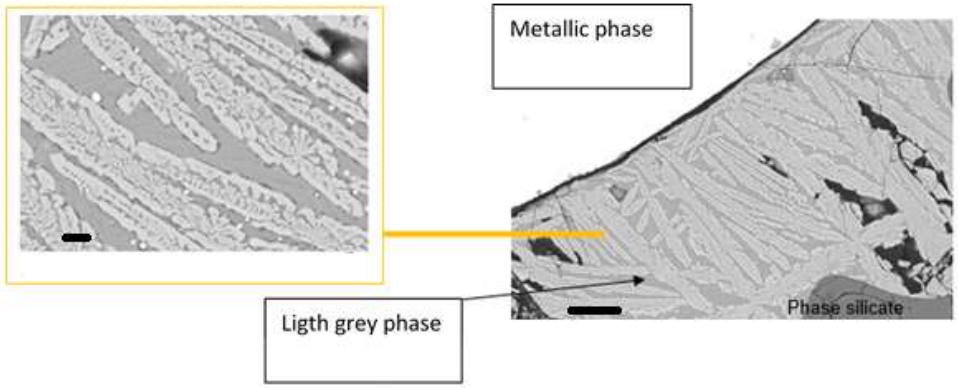

The analyses of the light grey phase enable the identification of an iron-enriched O-Na-Al-Si-Ca-Fe type corium phase with traces of K and of S.

The analyses of the whit dendritic phase enable the identification of an O-Na-Al-Si-Ca-Fe type corium phase with traces of K and of S, and a large proportion of Fe.

	O (wt%)	O (σwt%)	Na (wt%)	Na (σwt%)	Al (wt%)	Al (σwt%)	Si (wt%)	Si (σwt%)	K (wt%)	K (σwt%)	Ca (wt%)	Ca (σwt%)	Fe (wt%)	Fe (σwt%)	S (wt%)	S (σwt%)	Total (wt%)
Ligth grey phase	38.68	0.40	0.37	0.06	2.73	0.06	23.79	0.16	0.73	0.07	12.05	0.28	20.19	0.64	1.29	0.43	99.82
Dendritic phase	34.17	0.35	0.15	0.05	1.01	0.04	18.69	0.14	0.60	0.06	2.71	0.11	41.05	1.01	0.15	0.06	98.52

Conclusion

- Corium : heterogeneous and complex material (i.e geological material), Specific analytical procedure has to be developped through electron microscopy and X ray diffraction
- Quantitative analysis is allowed by WDS EPMA and light element can be measured like O, B, C.
- 3 study case of sever accident was analyzed (the distribution of boron in the in-vessel fuel debris, ICE corium, MCCI corium) and explained the material formation
- Diffraction methods give structural information

→ Combined Rietveld analysis with X ray and neutron diffraction accurate the determination of solid solution, this result are in good agreement with local EPMA microanalysis realized in the sample.

→ LAUE micro-diffraction : Interplay between composition fluctuations and stresses into crystals of uranium-zirconium and can show an increase of local deformation rate with the fast cooling.

→ EBSD can measured the formation of grain size during process

→ The new methodology can do determination of the relationship between corium cooling process and the cationic-anionic composition variation into the uranium-zirconium solid solutions in radioactive corium materials.

- Analytical approach through electron microscopy and diffraction methods and condition parameters could be transfered (i.e, F.P, M.A, Pu) in hot cell condition

Thank you for your attention!

IUMAS8 June 11-16, 2023 Banff, AB Canada

Thanks to :

Denis Menut scientist of MARS BEAM LINE at SOLEIL synchrotron

Emmanuelle Suard scientist of D2B at ILL

Jean Sébastien Micha scientist of BM32 at ESRF synchrotron

The authors gratefully thank the French Research Minister for the support to ICE- RSNR-Post-Fukushima program

CEA MARCOULE

30200 Bagnols sur Cèze

France

emmanuelle.brackx@cea.fr

Standard. + 33 4 66 33 92 54